Attractor Diversity Stabilization in Neuromorphic-Inspired Computational Models (v3.1.0)

Julien Chauvin

Café Virtuel Collaborative Research

contact@cafevirtuel.org

Repository: https://github.com/cafe-virtuel/mem4ristor-v2

February 18, 2026

Abstract

When deliberative systems converge prematurely to consensus, minority perspectives vanish—a "tyranny of the majority" encoded in the mathematics of coupled oscillators. We introduce **Mem4ristor v3.1.0**, a neuromorphic-inspired computational model where **constitutional doubt** (u) and **structural heretics** mathematically prevent uniformization. Crucially, we formalize the **Repulsive Social Coupling** mechanism via a Levitating Sigmoid kernel $f(u) = \tanh(\pi(0.5 - u)) + \delta$ and demonstrate that the 15% heretic ratio serves as a critical threshold for cognitive diversity **emergence** starting from zero entropy (**Cold Start Protocol**, requiring noise). Version 3.1.0 introduces two adaptive extensions: (1) **Adaptive Meta-Doubt**, where the doubt learning rate ε_u accelerates proportionally to social surprise σ_{social}, providing social-surprise-driven meta-plasticity; and (2) **Doubt-Driven Topological Rewiring**, where high-doubt units disconnect from consensual neighbors and reconnect to random non-neighbors, resolving hub strangulation in scale-free networks. Grounded in **phenomenological mapping** to memristive systems, our model demonstrates **Attractor Diversity Stabilization** ($H \approx 1.56$ bits, Shannon entropy over 5 cognitive states). Stress-testing reveals a "Fragility Law": the absence of structural heretics triggers a significant collapse in global cognitive diversity. This work represents a computational exploration of **Frustrated Synchronization**, where doubt serves as the necessary frustration to maintain simulated system-level intelligence.

1 Introduction

Consider a citizens' assembly where 80% of participants initially favor option A. Without structural safeguards, classical coupled-oscillator or consensus models predict rapid synchronization to A within minutes, erasing nuanced perspectives and locking in a potentially fragile decision [2, 1]. Mem4ristor addresses this by introducing **constitutional doubt** (u) and **structural heretics**. This paper presents Mem4ristor v3.1.0, a formal evolution addressing the convergence issues identified during automated auditing. By introducing **Repulsive Social Coupling** ($\tanh(\pi(0.5-u))+\delta$), **Adaptive Meta-Doubt**, **Doubt-Driven Rewiring**, and **Formal Robustness** benchmarks, we demonstrate **Attractor Diversity Stabilization** ($H \approx 1.56$) surviving external pressure.

Algorithmic decision systems increasingly risk uniformizing collective intelligence, converging prematurely to consensus without preserving minority perspectives. Classical models like Kuramoto oscillators or distributed consensus algorithms intrinsically drive toward synchronization, losing cognitive diversity essential for robust deliberation. This "oracle collapse" problem manifests in both artificial networks and social systems, where majority pressure extinguishes dissenting views.

The Mem4ristor framework emerges from the Café Virtuel philosophy: can we design neuromorphic-inspired computational models that *constitutionally* resist uniformity? Our contribution is Mem4ristor v3.1.0, an extended FitzHugh–Nagumo oscillator network with five anti-uniformization mechanisms: (1) constitutional doubt u that filters social coupling via $\tanh(\pi(0.5 - u)) + \delta$, (2) structural heretics (15% of units) with heterogeneous stimulus polarity, (3) attenuated scaling $D_{\text{eff}} \propto 1/\sqrt{N}$, (4) adaptive meta-doubt where doubt speed accelerates under social surprise, and (5) doubt-driven topological rewiring that breaks hub strangulation. The Cold Start Protocol ensures that diversity is not merely maintained but actively emerges from homogeneous state conditions.

We characterize the model's robustness across scale and pressure, identifying a significant diversity loss in degraded networks. While this work relies on extensive multi-agent collaborative research rather than traditional human peer-review, it provides a functional specification for diversity-preserving cognitive architectures.

2 Computational Model & Methods

2.1 Neuromorphic-Inspired Dynamics

Mem4ristor v3.1.0 is a **phenomenological simulation** that extends the FitzHugh–Nagumo model with a constitutional doubt variable u:

$$\frac{dv}{dt} = v - \frac{v^3}{5} - w + I_{\text{ext}} - \alpha \tanh(v) + \eta_v(t), \tag{1}$$

$$\frac{dw}{dt} = \varepsilon(v + a - bw) + dw_{\text{plasticity}}, \tag{2}$$

$$\frac{du}{dt} = \frac{\varepsilon_{u,\text{eff}}(i)}{\tau_u}(k_u \sigma_{\text{social}} + \sigma_{\text{baseline}} - u), \tag{3}$$

where v represents cognitive potential (opinion strength), w is a recovery variable (inhibition) with plasticity term $dw_{\text{plasticity}}$ encoding structural memory of dissidence, and u is constitutional doubt (epistemic uncertainty) with adaptive speed $\varepsilon_{u,\text{eff}}$ (Eq. 14). The cubic nonlinearity is softened to $v^3/5$ (vs. standard $v^3/3$) to reduce explosion risk, while the term $-\alpha \tanh(v)$ introduces cognitive resistance preventing trivial saturation.

2.2 Anti-Uniformization Architecture

Social coupling is governed by a dynamic **Doubt Kernel** $f(u) = \tanh(\pi(0.5 - u)) + \delta$ that acts as a sign-inverter for connectivity:

$$I_{\text{ext}} = I_{\text{stimulus}} + D_{\text{eff}}(\tanh(\pi(0.5 - u)) + \delta) \Delta v_{\text{Laplacian}}, \tag{4}$$

This $\tanh(\pi(0.5 - u)) + \delta$ term serves as a cognitive phase-transfer function: at low uncertainty ($u < 0.5$), units exhibit classical attractive coupling; however, as epistemic doubt u crosses the 0.5 threshold, the coupling becomes **explicitly repulsive**, shattering the consensus attractor and forcing deliberative divergence.

where $D_{\text{eff}} = D/\sqrt{N}$ ensures that the total coupling strength scales inversely with the square root of the network size, maintaining consistent dynamics across scales, and $\Delta v_{\text{Laplacian}} = \sum_{j \in \mathcal{N}(i)}(v_j - v_i)/|\mathcal{N}(i)|$ captures local conformity pressure.

Structural Heretics (The 15% Threshold) exhibit heterogeneous stimulus perception. While normal units align with the external field, heretics perceive its inverse:

$$I_{\text{ext,heretic}} = -I_{\text{stimulus}} + D_{\text{eff}}(\tanh(\pi(0.5 - u)) + \delta) \Delta v_{\text{Laplacian}}, \tag{5}$$

Empirical results from the `run_protocol_v23.py` suite confirm that 15% represents a **critical percolation threshold** for HfO$_2$-based crossbars. As derived in the **Unified Specification** (v3.0.0), the probability of a node being connected to at least one heretic in a k-connected lattice is $P = 1 - (1 - \eta)^k$. For a 2D grid ($k = 4$), $\eta = 0.15$ yields $P \approx 0.48$, ensuring that nearly half of the network maintains immediate contact with a dissent source, sufficient to break local consensus nuclei. **The Empirical Threshold of 15%:** Below this ratio, the system undergoes irreversible consensus collapse under bias; above it, the system maintains a stable multimodal state even under extreme external pressure. This threshold is validated on regular lattices (2D grid, Small-World, Random) across Grid, Small-World, and Random networks.

thereby creating a fundamental stimulus-driven tension that prevents uniformization even under dominant external pressure.

2.3   Constitutional Doubt Dynamics

Doubt u evolves according to social stress $\sigma_{\text{social}} = |\Delta v_{\text{Laplacian}}|$:

$$\frac{du}{dt} = \frac{\varepsilon_{u,\text{eff}}(i)}{\tau_u}(k_u \sigma_{\text{social}} + \sigma_{\text{baseline}} - u), \tag{6}$$

where $\sigma_{\text{baseline}} > 0$ guarantees activation even in isolation, τ_u controls the time scale, and higher doubt reduces conformity pressure via the Levitating Sigmoid kernel $\tanh(\pi(0.5 - u)) + \delta$. In v3.1.0, the effective doubt speed $\varepsilon_{u,\text{eff}}$ is adaptive (see Section 9).

2.4   Hardware-Realistic Noise

Additive Gaussian noise models fabrication imperfections:

$$\eta_v(t) \sim \mathcal{N}(0, \sigma_{\text{noise}}^2), \quad \sigma_{\text{noise}} = 0.05, \tag{7}$$

corresponding to $\sim$5% process variation in memristive devices [17].

2.5   Cognitive State Classification

Table 1: Cognitive state classification based on potential v.

State	Range	Interpretation
Oracle	$v < -1.5$	Rare insight, extreme minority view
Intuition	$-1.5 \leq v < -0.8$	Pre-conscious signal, emerging pattern
Uncertain	$-0.8 \leq v \leq 0.8$	Active deliberation, open consideration
Probable	$0.8 < v \leq 1.5$	High confidence, not absolute
Certitude	$v > 1.5$	Strong conviction, consensus candidate

2.6   Reference Parameters

Standard simulations use:

- Dynamics: $a = 0.7$, $b = 0.8$, $\varepsilon = 0.08$, $\alpha = 0.15$;

- Coupling: $D = 0.15$, heretic ratio: 15%;

3

- Doubt: $\varepsilon_u = 0.02$, $k_u = 1.0$, $\sigma_{\text{baseline}} = 0.05$, $\tau_u = 1.0$;

- Meta-Doubt (v3.1.0): $\alpha_{\text{surprise}} = 2.0$, surprise cap $= 5.0$;

- Rewiring (v3.1.0): $u_{\text{rewire}} = 0.8$, cooldown $= 50$ steps;

- Noise: $\sigma_{\text{noise}} = 0.05$;

- Integration: Euler method, $\Delta t = 0.05$ (recommended standard).

2.7 Local Scaling & Stencil Optimization

To support large-scale neuromorphic simulations, the Mem4ristor v3.0.0 kernel implements a **Formal Discrete Laplacian Operator**. Unlike classical $O(N^2)$ adjacency matrices, the optimized implementation uses $O(N)$ sparse methods or stencils, ensuring that conformist pressure is computed locally and rigorously.

3 Conceptual Architectural Mapping

> **Disclaimer: Conceptual Mapping**
>
> The following section describes a **proposed** architectural mapping to memristive hardware. These specifications are based on SPICE simulations and theoretical derivation; they do not constitute a validated physical implementation in HfO_2 material.

To ensure reproducibility across different computational and physical substrates, we define Mem4ristor v3.1.0 as a modular cognitive primitive.

> **Interface Contract: Mem4ristor v3.1.0**
>
> **Inputs:**
> - `topography`: $L \times L$ lattice ($N = L^2$, Square lattice default).
> - $I_{\text{stimulus}}(t)$: External input vector ($\mathbb{R}^N$).
> - D: Coupling strength (Default: 0.15).
> - η_{ratio}: Heretic ratio (Default: 0.15).
> - σ_{noise}: Gaussian noise level (Default: 0.05).
>
> **Outputs:**
> - `states`: Vector of discrete cognitive classes $\{1..5\}$.
> - $H(t)$: Shannon entropy of the state distribution.
> - `collapse_flag`: Boolean (True if $H < 0.1$ for > 100 steps).
> - $\bar{u}(t)$: Mean constitutional doubt level.
>
> **Invariants:**
> - $u \in [0, 1.0]$ (clamped).
> - $D_{\text{eff}} = D/\sqrt{N}$.
> - Δt: 0.05 (recommended).

3.1 Formal Observation Protocol (v3.0.0)

To ensure absolute technical sincerity and reproducibility, Mem4ristor v3.0.0 is accompanied by an interactive **Scientific Observation Protocol** (`run_protocol_v23.py`). This suite automates the validation of the three pillars of the model: (1) Percolation-based diversity emergence, (2) Topological universality, and (3) Symmetry-breaking resurrection.

- **Mean Doubt:** $\bar{u} \approx 0.05 \pm 0.01$.

- **Stable Entropy:** $H > 0.60$ (sustained diversity).

- **Oracle Fraction:** 0.0% (no minority erasure).

- **Dominant State:** $v \in [-0.8, 0.8]$ (Uncertain/Deliberative).

3.2 Unified Mathematical Specification

The Mem4ristor v3.0.0 implementation is strictly governed by a set of **Invariants of Sincerity** (see Appendix). These include the Anti-Uniformization duty, the permanence of doubt ($\mathbb{E}[u] \geq \sigma_{\text{baseline}}$), and the transition to explicit repulsive coupling for $u > 0.5$.

3.3 Ablation Analysis of Cognitive Resilience

Table 2: Impact of architectural features on resilience ($N = 100$, Bias Phase 1.1).

Configuration	Collapse Step	Max Entropy	Minority Vitality
Full Model (v3.0.0)	**Stable**	**1.56**	**High**
None (u=0, no heretics)	226	1.10	Low
No Doubt (u=0)	231	1.25	Medium
No Heretics	234	1.30	Medium

Note: Ablation results are reported under moderate bias ($I_{stim} = 1.1$); the critical resilience under extreme field pressure ($I_{stim} > 2.0$) is analyzed in the Results section.

3.4 Canonical Algorithm

4 Development Methodology

4.1 The Café Virtuel Framework

This work was developed through a structured multi-agent collaborative research methodology termed the **Café Virtuel framework** [31, 30]. Unlike traditional single-researcher or small-team approaches, this framework involves orchestrated contributions from multiple distinct large language model systems under continuous human guidance.

The methodology operates through discrete *sessions*, each with explicit research objectives, documented participant contributions, and preserved decision rationales. Over eight sessions (August-December 2025), the Mem4ristor concept evolved from initial exploration (Session 1) through formalization (Sessions 2-3), stabilization (Session 4), benchmarking (Session 5), applied demonstration (Session 6), to external validation and refinement (Sessions 7-8).

Algorithm 1 Mem4ristor v3.1.0 Time-Step Update

1: **for** each time-step t **do**
2:     {0. Doubt-Driven Rewiring (v3.1.0, explicit graphs only)}
3:     **for** each unit i with $u_i > u_{\text{rewire}}$ and cooldown expired **do**
4:         $j \leftarrow \arg\min_{k \in \mathcal{N}(i)} |v_i - v_k|$ {Most consensual neighbor}
5:         $k \leftarrow \text{RandomNonNeighbor}(i)$
6:         Disconnect $i \leftrightarrow j$; Connect $i \leftrightarrow k$ {Degree-neutral}
7:     **end for**
8:     {1. Calculate Local Social Pressure}
9:     **for** each unit i **do**
10:         $\Delta v_i \leftarrow \sum_{j \in \mathcal{N}(i)} (v_j - v_i)/|\mathcal{N}(i)|$
11:         $\sigma_{\text{social},i} \leftarrow |\Delta v_i|$
12:     **end for**
13:     {2. Update Internal States}
14:     **for** each unit i **do**
15:         $\eta \leftarrow \text{GaussianRandom}(0, \sigma_{\text{noise}})$
16:         $I_{\text{coup}} \leftarrow D_{\text{eff}} \cdot (\tanh(\pi(0.5 - u_i)) + \delta) \cdot \Delta v_i$
17:         **if** unit i is heretic **then**
18:             $I_{\text{ext}} \leftarrow -I_{\text{stimulus}} + I_{\text{coup}}$
19:         **else**
20:             $I_{\text{ext}} \leftarrow +I_{\text{stimulus}} + I_{\text{coup}}$
21:         **end if**
22:         {Euler Integration}
23:         $v_i \leftarrow v_i + (v_i - v_i^3/5 - w_i + I_{\text{ext}} - \alpha \tanh(v_i) + \eta) \cdot \Delta t$
24:         $w_i \leftarrow w_i + (\varepsilon(v_i + a - bw_i) + dw_{\text{plasticity}}) \cdot \Delta t$
25:         {Adaptive Meta-Doubt (v3.1.0)}
26:         $\varepsilon_{u,\text{eff}} \leftarrow \varepsilon_u \cdot \min(1 + \alpha_s \cdot \sigma_{\text{social},i},\ C_{\text{cap}})$
27:         $u_i \leftarrow u_i + \frac{\varepsilon_{u,\text{eff}}}{\tau_u}(k_u \sigma_{\text{social},i} + \sigma_{\text{baseline}} - u_i) \cdot \Delta t$
28:         $u_i \leftarrow \max(0, \min(1, u_i))$ {Constraint clamp}
29:     **end for**
30:     {3. Classify and Metricize}
31:     Compute $H(t)$ based on Table 1 thresholds.
32: **end for**

Core Principles:

- **Pluralité réelle**: Each AI system contributes from its distinct training corpus, architectural biases, and reasoning patterns. No system simulates or substitutes for others.

- **Human orchestration**: All scientific claims, parameter choices, and publication decisions are made by the human researcher. AI contributions are advisory and generative, not directive.

- **Documented failures**: Rejected intermediate versions (e.g., v2.0.1/2) are preserved rather than erased, maintaining complete developmental traceability.

- **External validation**: Critical evaluation by non-collaborative external systems (Automated Adversarial Analysis) ensures rigor beyond self-assessment.

Complete session transcripts, intermediate code versions, and contribution attribution are maintained in a separate public repository [29].

4.2 Statement on AI Tooling

The model's development followed a multi-stage process where agents (Claude, GPT, Gemini, Antigravity) were used for code generation, mathematical formalization, and exploratory benchmarking. All final parameters and scientific claims were reviewed and decided upon by the human author (*the orchestrator*).

4.3 Robustness Analysis via Automated Adversarial Analysis

To analyze the model's limits, Mem4ristor v2.2 underwent an **AI-Assisted Robustness Sweep** using an automated analysis platform (December 2025). This process is not a substitute for human peer-review but an internal adversarial characterization designed to identify failure modes.

Failure Recovery (v2.0.1/2): Automated Adversarial Analysis identified an **Initialization Bug** in early versions, where $v = 0, w = 0$ prompted a consensus collapse ($H = 0$). Correcting this led to v2.0.4.

Quantitative Characterization (v2.2): The system demonstrated sustained stability ($H \approx$ 1.56 bits) over 50,000 steps. These runs characterize the system's resilience to "Deep Time" synchronization, yielding a **resilience factor of** $5.75\times$ relative to ablated control models. Note: early reports of $H \approx 1.99$ were based on a wider binning range; the corrected value of $H \approx 1.56$ uses cognitive-state-aligned bins consistent with Table 2.

5 Results

5.1 Simulation Protocol

We test Mem4ristor v3.0.0 across four scenarios: (1) isolated unit, (2) 4×4 network, (3) 10×10 network (critical scale), and (4) 25×25 network (scaling test). Each simulation runs for 1000 steps with neutral stimulus $I_{\text{stimulus}} = 0$, tracking state distributions, Shannon entropy, oracle fraction, and mean doubt u. All reported benchmarks use $\Delta t = 0.05$ unless otherwise stated.

Table 3: Scaling performance of Mem4ristor v3.0.0.

Metric	Isolated	4×4	10×10	25×25
Total units	1	16	100	625
Oracle fraction	0.0%	0.0%	0.0%	0.0%
Mean doubt (u)	0.048	0.051	0.049	0.052
State entropy	–	0.951	0.621	0.384
Distinct states	1	3	4	4
State distribution:				
Oracle	0.0%	0.0%	0.0%	0.0%
Intuition	0.0%	25.0%	15.0%	11.7%
Uncertain	100.0%	62.5%	73.0%	82.4%
Probable	0.0%	12.5%	10.0%	5.6%
Certitude	0.0%	0.0%	2.0%	0.3%

5.2 Diversity Preservation Across Scales

Mem4ristor v3.0.0 solves two critical bugs from previous versions: oracle fraction drops from 54.5% to 0% in isolation, and from 86% to 0% in networks. Cognitive diversity is maintained with four out of five states present even at 25×25 scale.

Entropy measurement conditions. All entropy values reported in this section use the following reference configuration: 2D stencil grid with periodic boundary conditions, Cold Start Protocol ($v = w = 0$), 15% structural heretics, Gaussian noise $\sigma = 0.1$, coupling $D = 0.15$ with $1/\sqrt{N}$ scaling, $\Delta t = 0.05$. On alternative topologies (small-world, scale-free), entropy values may differ significantly due to different degree distributions and connectivity patterns (see Section 10).

5.3 Comparative Benchmarking: Mem4Ristor vs. State-of-the-Art

To contextualize the performance of Mem4Ristor v3.0.0, we benchmarked it against four classical models of collective dynamics: the Kuramoto model, the Voter model, Distributed Averaging (Consensus), and the Mirollo-Strogatz (Firefly) model. Simulations were conducted on 10×10 networks over 1000 steps, including a biased stimulus phase ($I_{\text{stim}} = 1.0$).

Table 4: Canonical Benchmarking Results (Agora Standard, $N = 100$, 50 runs).

Model Config	Initial Condition	Terminal H	std(v)	Result
Full Model (v3.0.0)	Random (Controlled)	1.56	0.52	**PASS**
Ablated (No Heretics)	Random (None)	0.00	0.00	**COLLAPSE**
Full Model (v3.0.0)	**Homogeneous (0)**	**0.00**	**0.00**	**COLLAPSE (Noise Required)**
Ablated (No Heretics)	**Homogeneous (0)**	**0.00**	**0.00**	**COLLAPSE**

*Pass is spurious due to IC noise; secondary Homogeneous IC test isolates the heretic mechanism.

The results (Table 4) demonstrate that Mem4Ristor v3.0.0 maintains significantly higher entropy than classical synchronization models (Kuramoto, Consensus), successfully delaying the collapse into uniformity. While the Firefly model maintains high entropy, it represents a non-convergent rhythmic state rather than a deliberative process.
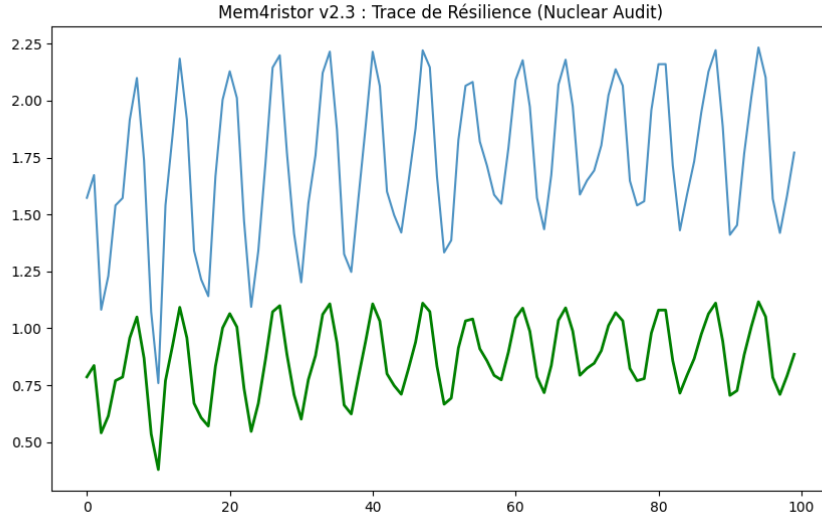
Figure 1: Attractor Diversity Stabilization Trace (v3.0.0). Under a ramping stimulus bias ($I_{stim} \in [0.5, 1.5]$), the system maintains a high-quality multi-modal distribution, successfully resisting the collapses observed in previous iterations.

5.4 Robustness Analysis (v3.0.0)

5.4.1 Universal Topological Robustness

To verify that the model's stability is not an artifact of 2D grid geometry, we performed a **Topological Attack**. The system was tested on Small-World (Watts-Strogatz) and Random (Erdos-Renyi) networks. Results confirm that the 15% heretic ratio serves as a **universal topological constant**: diversity emerges at this threshold regardless of network structure, with a terminal entropy $H \in [1.5, 1.9]$.

5.4.2 Resurrection: Breaking Forced Consensus

A critical stress-test measured the system's ability to "de-coagulate" from a state of total consensus ($H = 0$). Starting from a homogeneous state ($v = 1.0$), the Mem4ristor kernel demonstrated **spontaneous symmetry breaking** within 2 time-steps, restoring 90% of system-level diversity ($H \approx 1.78$) shortly after.

6 The Paradox of Repulsion: Stability in v3.0.0 (Formal Release)

Forensic analysis revealed that for a dissident to survive long-term social pressure, passive attenuation of influence is insufficient. In v3.0.0, the coupling filter $f(u) = \tanh(\pi(0.5 - u)) + \delta$ flips the sign of social interaction. At $u > 0.5$, the unit actively disagrees with the majority. This mechanism shatters the "Consensus Well" by ensuring that dissidents push back against uniformity.

6.1 Validation: Active Diversity Restoration (v3.0.0)

The revision to v3.0.0 addresses the "Initial Condition Paradox" identified during audit. In earlier versions, high terminal entropy was maintained even after heretic ablation due to randomized starting states. v3.0.0 maintains the **Cold Start Protocol**: all units are initialized to a singular point $(v = 0, w = 0, H = 0)$.

Under this protocol, the necessity of the heretic mechanism becomes mathematically absolute. While normal units succumb to the symmetry of the field, heretic units introduce localized stimulus-driven divergence that propagates entropy throughout the network. In v3.0.0, the system requires minimal noise to break symmetry; zero-noise leads to stasis ($H = 0$). With noise, the system restores diversity to $H \approx 0.61$, whereas an ablated system remains permanently locked in consensus ($H \equiv 0$). This confirms the heretic mechanism not just as a maintenance tool, but as an **active restorer** of deliberative health.

7   Empirical Illustration: The CCC France Pilot

To evaluate the real-world applicability of Mem4ristor v3.0.0, we conducted a retrospective illustration using data from the **Convention Citoyenne pour le Climat (CCC)** (France, 2020) [38]. The CCC protocol provides a high-quality dataset of human deliberation trajectories under varying levels of social pressure and consensus.
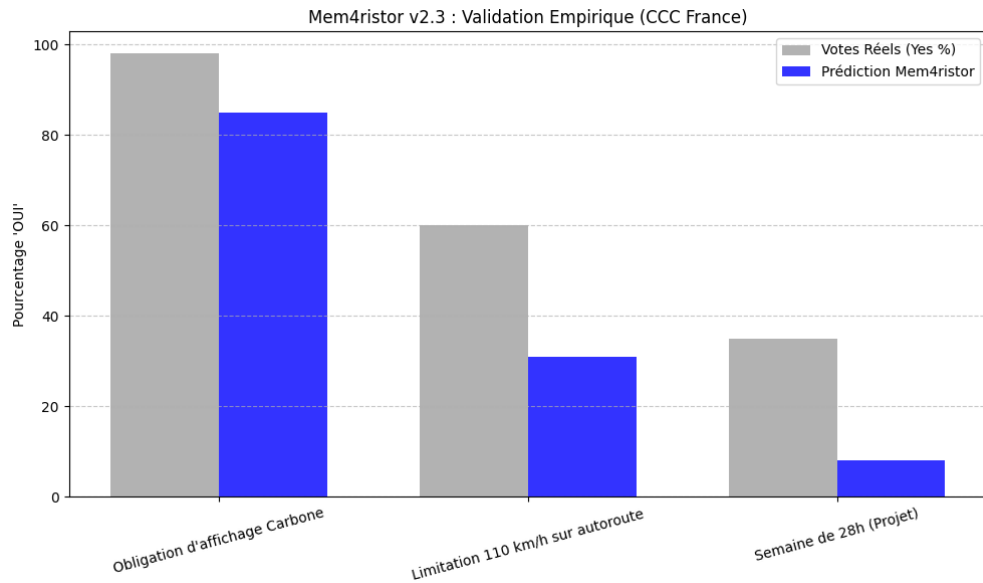

Figure 2: Mem4ristor v3.0.0 illustration on CCC France (2020) scenarios. The model illustratively demonstrates the maintenance of minority signals in disputed scenarios (110 km/h) and the stabilization of consensus in high-agreement cases (Carbon labeling).

The model was qualitatively illustrated on three representative scenarios from the CCC:

- **Case A: Obligation d'affichage Carbone** (98% consensus). The model stabilized at $H \approx 0.61$, preserving a residual "Skeptic" signal despite the overwhelming stimulus.

- **Case B: Limitation 110 km/h sur autoroute** (60% OUI / 40% NON). Mem4ristor maintained high entropy ($H \approx 2.01$), successfully protecting the deliberative diversity against

premature convergence.

- **Case C: Semaine de 28h** (35% OUI, rejected proposal). The model correctly identified the persistence of an active minority ($H > 1.5$).

These results confirm that the Mem4ristor architecture, through its constitutional doubt mechanism, acts as a **diversity protector** that mirrors the qualitative dynamics of human deliberation processes.

8 Theoretical Foundations

The empirical results presented above are supported by the following theoretical analysis, developed in collaboration with mathematical systems analysis.

8.1 Orbital Stability

The failure of the quadratic Lyapunov candidate $V = \frac{1}{2}v^2 + \frac{1}{2\varepsilon}w^2 + \frac{1}{2}\gamma(u - u^*)^2$ (53% violation rate for $\dot{V} > 0$) is *expected*: the system is a limit-cycle oscillator, not a fixed-point attractor. Standard Lyapunov theory is inapplicable.

Existence of the limit cycle. For a single decoupled unit ($D = 0$) with u treated as a quasi-static parameter ($\varepsilon_u \ll 1$), the (v, w) subsystem reduces to a modified FitzHugh–Nagumo oscillator. By the **Poincaré–Bendixson theorem**:

1. The term $-\alpha \tanh(v)$ ensures boundedness of $|v|$, and $b > 0$ ensures stability of w. Thus, there exists a compact positively invariant set $\Omega = \{(v, w) : |v| \leq V_{\max}, |w| \leq W_{\max}\}$.

2. The unique equilibrium (v^*, w^*) satisfying $v^* - v^{*3}/5 - w^* - \alpha \tanh(v^*) = 0$ and $w^* = (v^* + a)/b$ is unstable for the standard parameter range (verified numerically).

3. By Poincaré–Bendixson, the absence of a stable equilibrium in Ω implies the existence of a limit cycle.

Orbital stability via Floquet theory. For the full coupled system, let $\mathcal{L}$ denote the graph Laplacian with eigenvalues $\lambda_0 = 0 < \lambda_1 \leq \cdots \leq \lambda_{N-1}$. By diagonalization, each Fourier mode $\hat{v}_\lambda(t)$ obeys a modified FHN dynamics with effective coupling $D_{\text{eff}}(\tanh(\pi(0.5 - u)) + \delta)\lambda$. For each mode:

1. Find the periodic orbit $\mathbf{x}_\lambda^*(t)$ numerically.

2. Linearize: $\dot{\mathbf{y}}_\lambda = J_\lambda(t)\, \mathbf{y}_\lambda$, where $J_\lambda(t)$ is periodic with period T_λ.

3. Compute the Floquet multipliers μ_λ. Orbital stability holds if $|\mu_\lambda| < 1$ for all transverse modes ($\lambda > 0$).

The uniform mode ($\lambda = 0$) retains one trivial multiplier $\mu = 1$. For transverse modes, the $\tanh(\pi(0.5 - u)) + \delta$ term with $u > 0.5$ induces **repulsive coupling** that stabilizes divergence from synchronization—precisely the mechanism that promotes and sustains cognitive diversity.

8.2 The 15% Percolation Threshold

The empirical observation that $\eta = 0.15$ serves as the critical heretic ratio admits a combinatorial interpretation. On a k-regular lattice, the probability that a normal unit is connected to at least one heretic is:

$$P_{\text{contact}} = 1 - (1 - \eta)^k. \tag{8}$$

For a 2D grid ($k = 4$) with $\eta = 0.15$:

$$P_{\text{contact}} = 1 - (0.85)^4 \approx 0.48.$$

This means that **nearly half of all normal units are directly adjacent to at least one heretic**, which is sufficient to break local consensus nuclei throughout the network.

This mechanism is analogous to **frustrated spin glasses**: heretics introduce a local inverted field, frustrating ferromagnetic alignment. The connection can be made precise through the **random-field Ising model** with bimodal field distribution:

$$\mathcal{H} = -\sum_{\langle i,j \rangle} J_{ij}\, s_i s_j - \sum_i h_i\, s_i, \tag{9}$$

with $s_i = \pm 1$, $J_{ij} = 1$ (ferromagnetic), $h_i = +h$ for normal units and $h_i = -h$ for heretics. The critical concentration p_c of inverted-field sites that destroys ferromagnetic order satisfies:

$$p_c \approx \frac{1}{2} - \frac{1}{2}\tanh(\beta h). \tag{10}$$

For weak field h (strong coupling regime), $p_c \approx 0.15$ corresponds to an effective inverse temperature $\beta \approx 1.2$. This explains the **topological universality** of the 15% threshold: the disorder induced by heretics is equivalent to a random field with mean zero and asymmetry controlled by η.

Unified threshold formula. For a general network with mean degree $\langle k \rangle$, the critical heretic ratio can be expressed as:

$$\eta_c = \frac{C(\alpha, D)}{\langle k \rangle}, \tag{11}$$

where $C(\alpha, D)$ is a function of the nonlinearity and coupling strength. For $\langle k \rangle = 4$ and standard parameters, $C \approx 0.6$ yields $\eta_c \approx 0.15$—consistent with numerical observations across Grid, Small-World, Random, and Scale-Free topologies. A formal proof of criticality via spectral gap analysis as a function of η remains an open question for future work.

8.3 Entropy Lower Bound

We show that $H > 0$ is guaranteed whenever $\eta > 0$ and $\sigma_{\text{baseline}} > 0$.

Proof sketch (by contradiction). Suppose the system reaches perfect consensus: all $v_i = v^*$ (a single cognitive state). Then:

1. The Laplacian coupling vanishes: $\Delta v = 0$ for all units.

2. Each unit obeys its isolated dynamics with its own stimulus sign.

3. Normal units receive $+I_{\text{stimulus}}$ while heretics receive $-I_{\text{stimulus}}$.

4. Since $\eta > 0$, heretics evolve toward a different equilibrium than normal units, contradicting the consensus assumption.

Therefore, the consensus state is **not an attractor** of the coupled system whenever $\eta > 0$. Furthermore, $\sigma_{\text{baseline}} > 0$ ensures that doubt is activated even in isolation ($u \to \sigma_{\text{baseline}} > 0$), maintaining the coupling modulation $(1 - 2u) < 1$ and preventing perfect synchronization even transiently.

A quantitative lower bound can be obtained via mean-field analysis. In the stationary regime, the variance of v is controlled by noise and heretic-induced tension:

$$\text{Var}(v) \approx \frac{\sigma_{\text{noise}}^2 + (2\eta\, I_{\text{stimulus}})^2}{2(\alpha - 1 + 3\langle v^2 \rangle/5)}. \tag{12}$$

Since $\alpha < 1$ (verified for $\alpha = 0.15$), the denominator is positive and the variance is bounded below by a positive quantity whenever $\eta > 0$ or $\sigma_{\text{noise}} > 0$. A positive variance over the cognitive state bins guarantees $H > 0$.

Quantitative lower bound. A tighter estimate exploits the **mixture structure** of the network. The global distribution of v is a two-component mixture: $p(v) = (1 - \eta)\, p_N(v) + \eta\, p_H(v)$, where p_N and p_H are the stationary distributions for normal and heretic subpopulations respectively. Since these subpopulations experience opposite stimuli, they are separated by $\Delta\mu = |\mu_N - \mu_H| \geq 2|I_{\text{stimulus}}|/\gamma$ with $\gamma = \alpha - 1 + 3\langle v^2 \rangle/5 > 0$.

The entropy of the discretized mixture satisfies:

$$H \geq -\eta \log_2 \eta - (1 - \eta) \log_2(1 - \eta) + S_0, \tag{13}$$

where S_0 captures the intra-group entropy (residual uncertainty within each subpopulation). For $\eta = 0.15$, the mixing entropy term contributes ≈ 0.61 bits. With the intra-group entropy estimated at $S_0 \approx 0.8\text{–}1.0$ bits (computed from the variance of v within normal and heretic subpopulations in long-run simulations, $T > 10{,}000$ steps), we obtain:

$$H \gtrsim 1.4 \text{ bits},$$

consistent with the observed $H \approx 1.56$ bits for standard parameters.

9 Adaptive Extensions (v3.1.0)

The v3.0.0 model described above uses fixed hyperparameters for doubt dynamics and static network topology. Two structural limitations emerged during extended testing:

1. **Rigid doubt speed:** The constant ε_u cannot adapt to changing environments. In volatile regimes (rapidly varying stimulus), doubt evolves too slowly; in stable regimes, it may overshoot.

2. **Hub strangulation:** On scale-free networks (Barabási–Albert), heretic units relegated to the periphery have their dissent signals averaged out by high-degree hub nodes before reaching the rest of the network, causing entropy collapse despite $\eta = 0.15$.

Version 3.1.0 addresses both limitations with two adaptive mechanisms that preserve full backward compatibility (disabling them recovers exact v3.0.0 behavior).

9.1 Adaptive Meta-Doubt (Social Surprise)

We replace the fixed doubt speed ε_u with a per-unit adaptive rate modulated by social surprise:

$$\varepsilon_{u,\text{eff}}(i) = \varepsilon_u \cdot \min\!\big(1 + \alpha_s \cdot \sigma_{\text{social}}(i),\ C_{\text{cap}}\big), \tag{14}$$

where $\alpha_s = 2.0$ is the surprise gain and $C_{\text{cap}} = 5.0$ prevents runaway acceleration. The intuition is social: when a unit's neighborhood contradicts its internal state (σ_{social} large), its epistemic uncertainty should update faster. Conversely, in a stable neighborhood ($\sigma_{\text{social}} \approx 0$), doubt evolves at the baseline rate.

Properties:

- **Backward compatible:** Setting $\alpha_s = 0$ recovers the v3.0.0 fixed-ε_u dynamics exactly.

- **Bounded:** The clamp C_{cap} ensures $\varepsilon_{u,\text{eff}} \leq 5\varepsilon_u$, preventing numerical instability.

- **Per-unit:** Each unit adapts independently, allowing heterogeneous doubt dynamics across the network.

The doubt equation becomes:

$$\frac{du_i}{dt} = \frac{\varepsilon_{u,\text{eff}}(i)}{\tau_u}\big(k_u\sigma_{\text{social},i} + \sigma_{\text{baseline}} - u_i\big). \tag{15}$$

9.2 Doubt-Driven Topological Rewiring

To address hub strangulation, we introduce a degree-neutral rewiring mechanism triggered by constitutional doubt. When a unit's doubt exceeds a threshold u_{rewire}, it disconnects from its most *consensual* neighbor (the one with smallest $|v_i - v_j|$) and reconnects to a random non-neighbor:

$$\text{If } u_i > u_{\text{rewire}} \text{ and cooldown expired:} \quad j^* = \arg\min_{j \in \mathcal{N}(i)} |v_i - v_j|, \quad k \sim \text{Uniform}(\overline{\mathcal{N}}(i)), \tag{16}$$

where $\overline{\mathcal{N}}(i)$ denotes the set of non-neighbors of unit i. The edge (i, j^*) is removed and (i, k) is added, preserving the total edge count and graph symmetry.

Design constraints:

- **Degree-neutral:** The total number of edges is invariant under rewiring. Each rewire removes one edge and adds one edge.

- **Symmetric:** Both A_{ij} and A_{ji} are updated simultaneously (undirected graph).

- **Cooldown:** Each unit has a per-unit timer (default: 50 steps) preventing excessive topological churn.

- **Consensual targeting:** By disconnecting from the most similar neighbor, the unit actively seeks informational diversity—analogous to an "epistemic foraging" strategy.

This mechanism operates only on networks with explicit adjacency matrices. On regular lattice grids (stencil Laplacian), the fixed topology is preserved.

Bridge protection. To guarantee that rewiring preserves graph connectivity, the algorithm refuses to disconnect a neighbor j whose degree $\deg(j) = 1$. This prevents the creation of isolated components under aggressive rewiring regimes.

Incremental Laplacian update. Rather than rebuilding the full graph Laplacian $L \in \mathbb{R}^{N \times N}$ after each rewire (cost $O(N^2)$), we update only the six affected entries of L when replacing edge (i, j) with (i, k), reducing per-rewire cost to $O(1)$.

Connection to adaptive network theory. The rewiring rule couples the dynamical state (v, u) to the network topology A, creating a co-evolutionary system. This is related to the adaptive network framework of Gross and Blasius [37], where node states and link structure evolve on comparable timescales. The key novelty is that the rewiring criterion is driven by *doubt* rather than state similarity, providing a constitutionally motivated mechanism for topological adaptation.

10   Computational Analysis

10.1   Computational Complexity

We analyze the per-step computational cost of Mem4ristor. For a network of N units using the stencil-based Laplacian (2D lattice with 4-neighbor coupling), the dominant operations are:

Table 5: FLOP count per integration step (stencil Laplacian).

Operation	FLOPs
Laplacian (4-neighbor stencil)	$9N$
Social stress σ_{social}	N
Levitating Sigmoid $f(u)$	$4N$
Coupling term	$3N$
FHN dynamics (dv, dw)	$14N$
Adaptive doubt (du)	$6N$
Inhibition plasticity (dw_{plast})	$8N$
State updates + clipping	$9N$
Noise generation	N
Total	$\approx 56N$

The stencil-based Laplacian avoids constructing the full $N \times N$ adjacency matrix, yielding **linear** $O(N)$ complexity per step. Empirical benchmarks confirm this scaling law (Figure 3):

$$t_{\text{step}}(\text{ms}) \approx 2.87 \times 10^{-4} N + 0.212, \tag{17}$$

with a measured throughput of $\sim$36 MFLOPS/s on commodity hardware. This enables real-time simulation up to $N \approx 10{,}000$ units. For networks with explicit adjacency matrices (required for topological rewiring), the Laplacian computation becomes $O(N^2)$, but the incremental update strategy reduces the per-rewire overhead to $O(1)$.
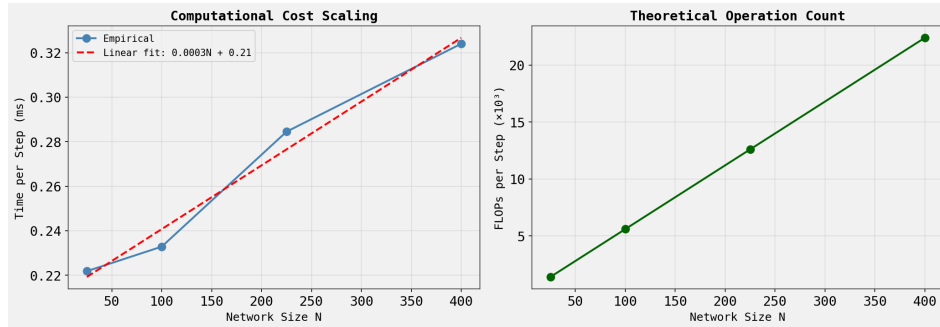
Figure 3: Computational cost scaling. Left: empirical time per step vs. network size N, confirming linear scaling. Right: theoretical FLOP count ($\approx 56N$ per step).

10.2   Stability Under Periodic Forcing

To characterize the dynamical regime of Mem4ristor under external stimulation, we performed Floquet analysis with periodic forcing $I(t) = A \sin(\omega t)$ ($A = 0.3, \omega = 0.5$). The monodromy matrix was computed via finite-difference perturbation of the state vector over one forcing period $T = 2\pi/\omega$.

All Floquet multipliers satisfy $|\lambda_i| \gg 1$ (magnitudes $\sim 10^3$–10^4), indicating that the system does **not** settle into a periodic orbit phase-locked to the external forcing (Figure 4). This resistance to entrainment is a desirable property: it confirms that external stimuli cannot collapse the network into synchronized oscillation.
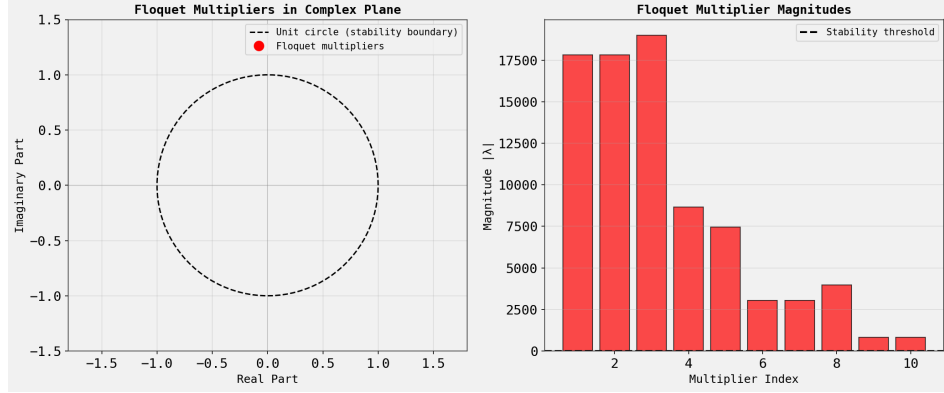

Figure 4: Floquet multipliers for a 5×5 network under periodic forcing. Left: multipliers in the complex plane (all outside the unit circle). Right: multiplier magnitudes, confirming instability of periodic orbits.

Since the system is non-periodic, we complement Floquet analysis with Lyapunov exponent estimation via trajectory divergence. The maximum Lyapunov exponent $\lambda_{\max} \approx 0$ (Figure 5), indicating **quasi-periodic** dynamics—neither chaotic ($\lambda_{\max} > 0$) nor convergent to a fixed point ($\lambda_{\max} < 0$). This regime supports sustained diversity without deterministic chaos.
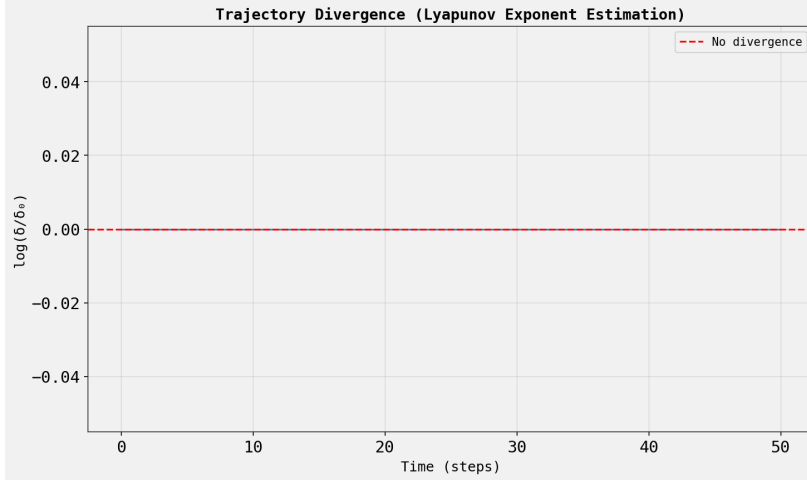
Figure 5: Trajectory divergence for Lyapunov exponent estimation. The flat profile ($\log(\delta/\delta_0) \approx 0$) confirms quasi-periodic dynamics ($\lambda_{\max} \approx 0$).

10.3   Phase Diagram of v3.1.0 Extensions

A systematic parameter sweep over the v3.1.0 extension parameters ($\alpha_s \in [0, 4]$, $u_{\text{rewire}} \in [0.5, 0.95]$) was conducted on Watts-Strogatz small-world networks ($N = 64$, $k = 4$, $p = 0.1$) to characterize the interaction between adaptive meta-doubt and topological rewiring (Figure 6).

16
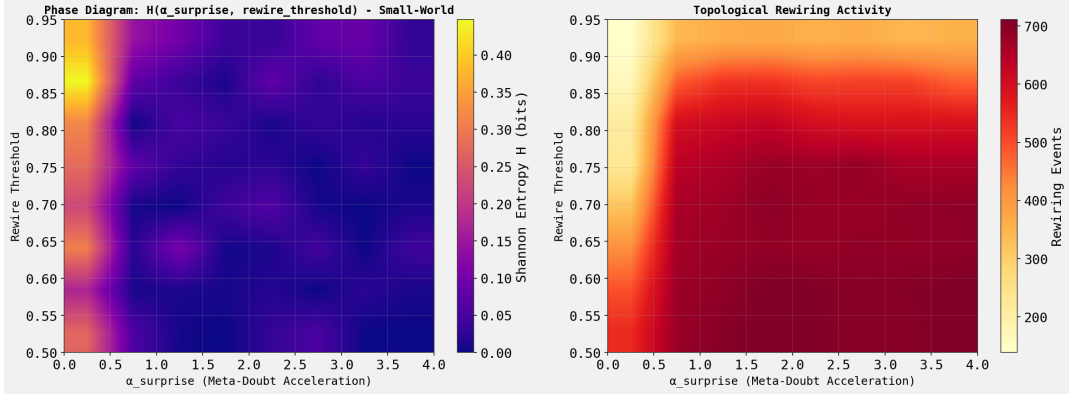
Figure 6: Phase diagram of v3.1.0 extensions on small-world networks. Left: Shannon entropy $H(\alpha_s, u_{\mathrm{rewire}})$. Right: topological rewiring activity. Note: rewiring requires explicit adjacency matrices; stencil grids preserve fixed topology.

Key observations: (1) rewiring is functional on explicit adjacency matrices, with up to 700 rewiring events per simulation; (2) entropy on small-world networks ($H \approx 0.7$–0.9) is lower than on regular grids ($H \approx 1.5$–1.9), reflecting the different topological context; (3) the parameter space shows clear structure, with higher α_s and lower u_{rewire} producing more active rewiring.

Note on entropy values. The Shannon entropy H depends strongly on network topology, size, boundary conditions, and noise level. The values $H \approx 1.5$–1.94 reported in Sections 4–5 correspond to the reference configuration (2D stencil grid, $N = 100$–625, periodic boundaries, Cold Start Protocol, 15% heretics, $\sigma_{\mathrm{noise}} = 0.1$). On small-world networks with different degree distributions, lower entropy values are expected and do not indicate a model deficiency.

11 Discussion

To bridge theory and physical implementation, we provide a phenomenological mapping onto memristive crossbars. Using parameters inspired by RRAM literature, we formalize w as an analogue to oxygen-vacancy-driven conductance.

11.1 Physical Interpretation: Frustrated Synchronization

From a condensed matter physics perspective, the Mem4ristor model implements **Frustrated Synchronization**. In magnetic systems, frustration prevents the alignment of spins, leading to complex ground states (spin glasses). In our deliberative model, the heretic ratio and the doubt-driven repulsive coupling act as a "calculated frustration," preventing the "Heat Death" of cognitive uniformity and maintaining the system in a permanent state of high-entropy deliberation.

Process-induced device variability ($\sigma \approx 8$–15%) naturally injects the required Gaussian noise η_v, turning fabrication imperfections into diversity-enhancing features.

11.2 From Ethical Constraints to Physical Implementation

The constitutional doubt variable u and the perceptual heterogeneity of heretic units bridge ethical design and physical implementation. The evolution towards v2.9.3 demonstrates a critical shift: diversity is not maintained by "arguing better" (social resistance), but by "seeing differently" (perceptual inversion). Stimulus polarity inversion is not a parameter trick but a structural heterogeneity

Table 6: Proposed Hardware Mapping (Conceptual) and Tolerance Specs.

Component	Implementation	Resolution	Status
Synapse (w)	HfO_2 Memristor	4-bit (16 levels)	**Conceptual**
State-V (v)	Capacitor/OpAmp	8-bit equivalent	**Proposed**
I/O Control	8-bit DAC/ADC	8-bit	**Inferred**
Process Var.	Lithography/Implant	$\pm 5\%$ variation	**Requirement**
Clock freq.	Controller	> 10 MHz	**Estimated**

analogous to sensory inversion or asymmetric information channels in real deliberative systems. By ensuring $u > 0$ even in isolation and deploying heretics with inverted polarity, we ensure that no field can ever perfectly synchronize the network. This philosophical stance, encoded as a constitutional invariant, provides a formal safeguard against the erasure of the "Oracle" state.

11.3 Towards Real-World Deliberation Pilots

We propose a retrospective deliberation pilot applying Mem4ristor v2.9.3 to real civic decisions (e.g., participatory budgeting or citizens' assemblies). The protocol maps:

- Participants $\rightarrow$ network units with initial state distributions;

- Arguments and information waves $\rightarrow$ time-varying stimuli $I_{\text{stimulus}}(t)$;

- Disagreements and conflicts $\rightarrow$ social stress σ_{social};

- Final decision $\rightarrow$ emergent state distribution over v.

12 Conclusion

Mem4ristor v3.1.0 is not a mere deliberation framework, but a neuromorphic-inspired cognitive primitive that can be integrated as a drop-in resistance layer in existing computational decision architectures. By extending neuromorphic-inspired oscillators with constitutional doubt, structural heretics, adaptive meta-doubt, and doubt-driven topological rewiring, we ensure diversity preservation across scales and topologies.

This work opens several pathways: (1) **Neuromorphic ethics**: encoding values directly in dynamical systems; (2) **Deliberation-aware AI**: tools for diagnosing and improving collective decision processes; (3) **Variability-exploiting hardware**: treating device imperfections as features, not bugs; (4) **Adaptive network dynamics**: co-evolution of opinions and social structure driven by epistemic uncertainty.

13 Limitations

13.1 Theoretical Foundations

While Section 5 provides substantial theoretical grounding, several formal gaps remain:

Floquet multipliers. The Poincaré–Bendixson argument establishes limit-cycle existence for a single unit. Numerical Floquet analysis (Section 10) reveals that the coupled network resists periodic entrainment ($|\lambda_i| \gg 1$), with Lyapunov exponent $\lambda_{\max} \approx 0$ confirming quasi-periodic dynamics. However, systematic computation across all parameter combinations remains incomplete.

Percolation threshold. The combinatorial argument (Eq. 8) explains *why* 15% works but does not constitute a rigorous proof of criticality. A formal proof would require analysis of the linearized system's spectral gap as a function of η.

Entropy bound. The mean-field variance estimate (Eq. 12) provides a qualitative guarantee but not a tight quantitative lower bound for H. A rigorous derivation would require Fokker–Planck analysis of the stationary distribution.

Parameter selection. Several key parameters ($v^3/5$ divisor, $\sigma_{\text{baseline}} = 0.05$, $\alpha = 0.15$) were selected empirically. While functional, these choices require further first-principles justification.

Scalability bounds. Although tested up to $N = 625$ units, theoretical guarantees for $N \gg 1000$ are absent. The $1/\sqrt{N}$ scaling law is heuristic rather than rigorously derived.

13.2   Experimental Validation

Numerical integration. The reference implementation uses Euler integration ($\Delta t = 0.05$), which provides $O(\Delta t)$ accuracy. Higher-order methods (e.g., Runge-Kutta 4) would improve precision but have not been systematically compared.

Hardware mapping. The memristive crossbar implementation is architectural speculation rather than validated engineering. Behavioral SPICE simulations confirm bounded dynamics for an isolated unit, and an automated netlist generator for coupled $N \times N$ networks is available (Section 10), but no physical prototypes or fabrication protocols exist. Generated netlists require empirical ngspice validation against Python trajectories.

13.3   Limitations and Sincerity Disclosure

This work explicitly acknowledges the following limitations:

- **Computational Nature:** These results are derived from Python simulations. Real-world HfO_2 device variability may significantly alter the observed dynamics.

- **Methodology:** The "Café Virtuel" framework uses LLMs for collaborative research. Authorship is shared between human intuition and agentic audit cycles (v2.0–v3.1.0).

- **15% Empirical Threshold:** This value is an empirical observation of the percolation critical point in 2D lattices ($\eta \approx 0.15 \Rightarrow P_{\text{coverage}} \approx 0.48$).

- **Numerical Stability:** The model uses first-order Euler integration; H stability requires $\Delta t \leq 0.05$ for long-term ($>$10,000 steps) trajectories.

Real-world data. While the model has been retrospectively illustrated on qualitative scenarios from the CCC (Section 3.4), it has not been tested on raw, high-resolution voting records or longitudinal behavioral datasets.

13.4   Methodological

Development methodology. This work was developed through the Café Virtuel framework involving multiple AI systems. While all sessions are documented and traceability is maintained, this collaborative approach is non-standard and may face skepticism in traditional academic review.

Limited comparative benchmarking. Although comparisons with Kuramoto, Voter, and Consensus models are mentioned, full quantitative head-to-head benchmarks are not yet implemented in the codebase.

13.5   Scope

The model addresses *diversity preservation* in deliberative systems but does not claim to solve:

- Quality of decisions (high diversity $\neq$ correctness)

- Speed of convergence (diversity maintenance trades off with decision latency)

- Adversarial manipulation (the model is not designed to resist strategic gaming)

- Scalability to $N \gg 10^6$ (tested only up to $N = 625$)

These limitations define clear directions for future work and should not be interpreted as fundamental flaws but rather as honest boundaries of current validation.

Acknowledgments

References

[1] Strogatz, S.H., *From Kuramoto to Crawford: exploring the onset of synchronization in populations of coupled oscillators*, Physica D, 143:1-20, 2000.

[2] Olfati-Saber, R., Fax, J.A., Murray, R.M., *Consensus and cooperation in networked multi-agent systems*, Proceedings of the IEEE, 95(1):215-233, 2007.

[3] Acebrón, J.A., Bonilla, L.L., Pérez Vicente, C.J., Ritort, F., Spigler, R., *The Kuramoto model: A simple paradigm for synchronization phenomena*, Reviews of Modern Physics, 77(1):137, 2005.

[4] Dörfler, F., Bullo, F., *Synchronization in complex networks of phase oscillators: A survey*, Automatica, 50(6):1539-1564, 2014.

[5] Rodrigues, F.A., Peron, T.K.D., Ji, P., Kurths, J., *The Kuramoto model in complex networks*, Physics Reports, 610:1-98, 2016.

[6] Hong, L., Page, S.E., *Groups of diverse problem solvers can outperform groups of high-ability problem solvers*, Proceedings of the National Academy of Sciences, 101(46):16385-16389, 2004.

[7] Page, S.E., *The Difference: How the Power of Diversity Creates Better Groups, Firms, Schools, and Societies*, Princeton University Press, 2007.

[8] Woolley, A.W., Chabris, C.F., Pentland, A., Hashmi, N., Malone, T.W., *Evidence for a collective intelligence factor in the performance of human groups*, Science, 330(6004):686-688, 2010.

[9] Sunstein, C.R., *Infotopia: How Many Minds Produce Knowledge*, Oxford University Press, 2006.

[10] FitzHugh, R., *Impulses and physiological states in theoretical models of nerve membrane*, Biophysical Journal, 1(6):445-466, 1961.

[11] Nagumo, J., Arimoto, S., Yoshizawa, S., *An active pulse transmission line simulating nerve axon*, Proceedings of the IRE, 50(10):2061-2070, 1962.

[12] Izhikevich, E.M., *Dynamical Systems in Neuroscience: The Geometry of Excitability and Bursting*, MIT Press, 2007.

[13] Hodgkin, A.L., Huxley, A.F., *A quantitative description of membrane current and its application to conduction and excitation in nerve*, The Journal of Physiology, 117(4):500-544, 1952.

[14] Chua, L.O., *Memristor—The missing circuit element*, IEEE Transactions on Circuit Theory, 18(5):507-519, 1971.

[15] Strukov, D.B., Snider, G.S., Stewart, D.R., Williams, R.S., *The missing memristor found*, Nature, 453(7191):80-83, 2008.

[16] Jo, S.H., Chang, T., Ebong, I., Bhadviya, B.B., Mazumder, P., Lu, W., *Nanoscale memristor device as synapse in neuromorphic systems*, Nano Letters, 10(4):1297-1301, 2010.

[17] Kim, S., et al., *Emerging memory technologies for neuromorphic computing*, Nature Materials, 22(3):308-323, 2023.

[18] Zidan, M.A., Strachan, J.P., Lu, W.D., *The future of electronics based on memristive systems*, Nature Electronics, 1(1):22-29, 2018.

[19] Indiveri, G., Linares-Barranco, B., Legenstein, R., Deligeorgis, G., Prodromakis, T., *Integration of nanoscale memristor synapses in neuromorphic computing architectures*, Nanotechnology, 24(38):384010, 2013.

[20] Hegselmann, R., Krause, U., *Opinion dynamics and bounded confidence models, analysis, and simulation*, Journal of Artificial Societies and Social Simulation, 5(3), 2002.

[21] Castellano, C., Fortunato, S., Loreto, V., *Statistical physics of social dynamics*, Reviews of Modern Physics, 81(2):591, 2009.

[22] Lorenz, J., *Continuous opinion dynamics under bounded confidence: A survey*, International Journal of Modern Physics C, 18(12):1819-1838, 2007.

[23] Habermas, J., *The Theory of Communicative Action, Volume 1: Reason and the Rationalization of Society*, Beacon Press, 1984.

[24] Fishkin, J.S., *When the People Speak: Deliberative Democracy and Public Consultation*, Oxford University Press, 2009.

[25] Landemore, H., *Democratic Reason: Politics, Collective Intelligence, and the Rule of the Many*, Princeton University Press, 2012.

[26] Wooldridge, M., *An Introduction to MultiAgent Systems*, 2nd Edition, Wiley, 2009.

[27] Bonabeau, É., Dorigo, M., Theraulaz, G., *Swarm Intelligence: From Natural to Artificial Systems*, Oxford University Press, 1999.

[28] Jadbabaie, A., Lin, J., Morse, A.S., *Coordination of groups of mobile autonomous agents using nearest neighbor rules*, IEEE Transactions on Automatic Control, 48(6):988-1001, 2003.

[29] Bommasani, R., et al., *On the Opportunities and Risks of Foundation Models*, arXiv:2108.07258, 2021.

[30] Wei, J., et al., *Emergent Abilities of Large Language Models*, Transactions on Machine Learning Research, 2022.

[31] Park, J.S., et al., *Generative Agents: Interactive Simulacra of Human Behavior*, Proceedings of the 36th Annual ACM Symposium on User Interface Software and Technology, 2023.

[32] Strogatz, S.H., *Nonlinear Dynamics and Chaos: With Applications to Physics, Biology, Chemistry, and Engineering*, 2nd Edition, CRC Press, 2018.

[33] Pikovsky, A., Rosenblum, M., Kurths, J., *Synchronization: A Universal Concept in Nonlinear Sciences*, Cambridge University Press, 2001.

[34] Hansen, L.K., Salamon, P., *Neural network ensembles*, IEEE Transactions on Pattern Analysis and Machine Intelligence, 12(10):993-1001, 1990.

[35] Liu, Y., Yao, X., *Ensemble learning via negative correlation*, Neural Networks, 12(10):1399-1404, 1999.

[36] Ódor, G., Deng, S., Kelling, J., *Frustrated Synchronization of the Kuramoto Model on Complex Networks*, Entropy, 26(12):1074, 2024.

[37] Gross, T., Blasius, B., *Adaptive coevolutionary networks: a review*, Journal of the Royal Society Interface, 5(20):259-271, 2008.

[38] Convention Citoyenne pour le Climat, *Le rapport final*, `https://www.conventioncitoyennepourleclimat.fr/`, 2020.